

# ANALYSIS OF SEGMENTATION TECHNIQUES ON FOOT ULCER IMAGES

**A.Suresh<sup>1</sup>, S. Lavanya<sup>2</sup>**

<sup>1</sup>Department of ECE, M.R.I.T.S, Hyderabad, (India)

<sup>2</sup>Assistant Professor Department of ECE, M.R.I.T.S, Hyderabad, (India)

## ABSTRACT

*The main objective of this paper is to implement the Chan-Vese active contour based method for medical purpose to easily identifying of ulcer affected area in a foot of a diabetic patient. Chan-Vese active contour method was used for segmentation. This method took into account as of visualization of the diabetic ulcers in the foot and used segmentation and represented with effective ulcer area with colour and also in grey colour images. In previous methods the ulcers are identified by ultrasound images using segmentation techniques but this method have disadvantages are noisier and have poorer image quality than other imaging modalities like CT or MRI and hence require an experienced clinician for interpretation, ultrasound images,*

**Keywords: Chan-Vese, CT Images, Diabetic Ulcers, MRI Images, Segmentation.**

## I. INTRODUCTION

Diabetes mellitus affects 194 million people worldwide<sup>1</sup> and is expected to increase in prevalence to 439 million by the year 2030.<sup>2</sup> Foot ulceration is a major complication that occurs in as many as 15–25% of type 1 and 2 patients with diabetes mellitus over their lifetime.<sup>3, 4</sup> If left untreated, foot ulcers may become infected and develop deep tissue necrosis, which may require amputation.<sup>5</sup> In fact, foot ulcers precede roughly 85% of all lower extremity amputations in patients with diabetes mellitus<sup>5</sup> and more than 88×10<sup>3</sup> lower limb amputations are performed annually on diabetic patients in the United States. The cost of foot disorder diagnosis and management is estimated to be >\$6 billion annually in the United States.<sup>7, 8</sup> Furthermore, it has been suggested that 40%–85% of diabetic foot amputations can be avoided with early detection and preventive techniques such as offloading and improved hygiene.<sup>9</sup> Automated early identification of tissue at risk of ulcerating may enable directed care, thereby reducing the incidence of foot ulceration and amputation. This study proposes to use hyperspectral imaging as a screening tool for detecting tissue at risk of diabetic foot ulcers before tissue damages become apparent to a care giver in a clinical setting.

### 1.1 Diabetic Foot Ulcers

Prolonged and poorly controlled diabetes irreparably damages bodily tissues. Nerve damage in the lower limbs results in diabetic neuropathy, whereby the patient's somatosensory and autonomic function are diminished or completely lost.<sup>10</sup> The subsequent loss of protective sensation, impaired gait control, bone deformities (e.g.,

Charcot foot), callus formation, and/or inhibited sweat response result in excessive shear and pressure that damages the diabetic foot.<sup>10, 11</sup> Furthermore, 10–40% of diabetic patients are afflicted with peripheral vascular disease.<sup>12</sup> Typically, the vessels that carry blood to the legs, arms, stomach, or kidneys narrow due to inflammation or tissue damage, resulting in impaired blood flow. Thus, repeated trauma to the foot in conjunction with inhibited protective or healing response due to denervation and/or poor vascularization increases the risk of foot ulceration in diabetic patients.

## 1.2 Medical Hyper Spectral Imaging

Hyper spectral imaging consists of recording a series of images representing the intensity of diffusely reflected light from biological tissue at discrete wavelengths  $\lambda_j$ .<sup>13</sup> The resulting set of images is called a hypercube, denoted by  $H(x, y, \lambda_j)$ , where  $x$  and  $y$  are the two spatial coordinates and  $\lambda_j$  is the spectral coordinate. Each pixel in a hypercube corresponds to the diffuse reflectance spectrum of the tissue at a location  $(x, y)$ . Analysis of the hypercube can reveal the local concentration of tissue chromophores, such as melanin or hemoglobin.<sup>13, 14</sup> Hemoglobin is the molecule in blood responsible for oxygen transport from the lungs to the rest of the body. In its oxygen-bounded and unbounded forms, hemoglobin is called oxyhemoglobin and deoxyhemoglobin, respectively. The ratio of oxyhemoglobin concentration to the total hemoglobin concentration in the blood is the so-called oxygen saturation denoted by  $SO_2$ . It indicates the rate of oxygen delivery to and consumption by the tissues. The optical extinction coefficient of oxyhemoglobin differs significantly from that of deoxyhemoglobin.<sup>15</sup> Thus, the spectral absorption coefficient of tissue depends on the concentration and oxygen saturation of hemoglobin within the tissue. Furthermore, changes in the tissue's spectral absorption coefficient change its diffuse reflectance spectrum. Thus, using the hyper spectral imaging technique, known as transcutaneous tissue oximetry, it is possible to estimate the hemoglobin concentration and oxygen saturation from the tissue's diffuse reflectance. Recently, hyper spectral imaging in the visible and near infrared parts of the spectrum has been used to determine the spatial distribution of oxygen saturation in human skin<sup>13, 16, 17</sup> and to detect the circulatory changes in the diabetic foot.<sup>18–20</sup> Nouvong et al.<sup>18</sup> enrolled 66 type 1 and type 2 diabetic subjects and followed them for up to 18 months. Nouvong et al.<sup>18</sup> evaluated hyper spectral imaging as a tool for predicting the healing potential of diabetic foot ulcers. In brief, 54 of the enrolled subjects completed the study. Each subject had one or more diabetic foot ulcer(s) at the beginning of the study. Hyper spectral tissue oximetry measurements of these subjects' feet were performed every two weeks for up to 18 months or until the ulcer healed. Then, ulcers were manually classified into one of two groups namely (i) ulcers that healed within 24 weeks and (ii) ulcers that did not heal within 24 weeks. Periwound averaged oxyhemoglobin and deoxyhemoglobin concentrations as well as oxygen saturation were calculated around nonhealing ulcers and found, on average, to be respectively 25, 6.8, and 10% smaller than those estimated around healing ulcers

## II. IMAGE SEGMENTATION

In computer vision, image segmentation is the process of partitioning a digital image into multiple segments (sets of pixels, also known as super pixels). The goal of segmentation is to simplify and/or change the representation of an image into something that is more meaningful and easier to analyze. Image segmentation is typically used to locate objects and boundaries (lines, curves, etc.) in images. More precisely, image segmentation is the process of assigning a label to every pixel in an image such that pixels with the same label

share certain visual characteristics. The result of image segmentation is a set of segments that collectively cover the entire image, or a set of contours extracted from the image (see edge detection). Each of the pixels in a region is similar with respect to some characteristic or computed property, such as color, intensity, or texture. Adjacent regions are significantly different with respect to the same characteristics. When applied to a stack of images, typical in medical imaging, the resulting contours after image segmentation can be used to create 3D reconstructions with the help of interpolation algorithms like marching cubes.

## 2.1 Clustering Methods

The K-means algorithm is an iterative technique that is used to partition an image into K clusters. The basic algorithm is:

1. Pick  $K$  cluster centers, either randomly or based on some heuristic
2. Assign each pixel in the image to the cluster that minimizes the distance between the pixel and the cluster center
3. Re-compute the cluster centers by averaging all of the pixels in the cluster
4. Repeat steps 2 and 3 until convergence is attained (e.g. no pixels change clusters)

In this case, distance is the squared or absolute difference between a pixel and a cluster center. The difference is typically based on pixel color, intensity, texture, and location, or a weighted combination of these factors.  $K$  can be selected manually, randomly, or by a heuristic. This algorithm is guaranteed to converge, but it may not return the optimal solution. The quality of the solution depends on the initial set of clusters and the value of  $K$ .

## 2.2 Compression Based Methods

Compression based methods postulate that the optimal segmentation is the one that minimizes, over all possible segmentations, the coding length of the data. The method describes each segment by its texture and boundary shape. Each of these components is modeled by a probability distribution function and its coding length is computed as follows:

1. The boundary encoding leverages the fact that regions in natural images tend to have a smooth contour. This prior is used by Huffman coding to encode the difference chain code of the contours in an image. Thus, the smoother a boundary is, the shorter coding length it attains.

2. Texture is encoded by lossy compression in a way similar to minimum description length (MDL) principle, but here the length of the data given the model is approximated by the number of samples times the entropy of the model. The texture in each region is modeled by a multivariate normal distribution whose entropy has closed form expression. An interesting property of this model is that the estimated entropy bounds the true entropy of the data from above. This is because among all distributions with a given mean and covariance, normal distribution has the largest entropy. Thus, the true coding length cannot be more than what the algorithm tries to minimize.

## 2.3 Histogram Based Methods

Histogram-based methods are very efficient when compared to other image segmentation methods because they typically require only one pass through the pixels. In this technique, a histogram is computed from all of the pixels in the image, and the peaks and valleys in the histogram are used to locate the clusters in the image. Color or intensity can be used as the measure.

## 2.4 Edge Detection Methods

Edge detection is a well-developed field on its own within image processing. Region boundaries and edges are closely related, since there is often a sharp adjustment in intensity at the region boundaries. Edge detection techniques have therefore been used as the base of another segmentation technique. The edges identified by edge detection are often disconnected. To segment an object from an image however, one needs closed region boundaries. The desired edges are the boundaries between such objects. Segmentation methods can also be applied to edges obtained from edge detectors. Lindeberg and Li developed an integrated method that segments edges into straight and curved edge segments for parts-based object recognition, based on a minimum description length (MDL) criterion that was optimized by a split-and-merge-like method with candidate breakpoints obtained from complementary junction cues to obtain more likely points at which to consider partitions into different segments.

## 2.5 Region Growing Methods

The first region-growing method was the seeded region growing method. This method takes a set of seeds as input along with the image. The seeds mark each of the objects to be segmented. The regions are iteratively grown by comparing all unallocated neighboring pixels to the regions. The difference between a pixel's intensity value and the region's mean,  $\delta$ , is used as a measure of similarity. The pixel with the smallest difference measured this way is allocated to the respective region. This process continues until all pixels are allocated to a region. Seeded region growing requires seeds as additional input. The segmentation results are dependent on the choice of seeds. Noise in the image can cause the seeds to be poorly placed. Unseeded region growing is a modified algorithm that doesn't require explicit seeds. It starts off with a single region  $A_1$  – the pixel chosen here does not significantly influence final segmentation. At each iteration it considers the neighboring pixels in the same way as seeded region growing. It differs from seeded region growing in that if the minimum  $\delta$  is less than a predefined threshold  $T$  then it is added to the respective region  $A_j$ . If not, then the pixel is considered significantly different from all current regions  $A_i$  and a new region  $A_{n+1}$  is created with this pixel. A special region-growing method is called  $\lambda$ -connected segmentation (see also lambda-connectedness). It is based on pixel intensities and neighborhood-linking paths. A degree of connectivity (connectedness) will be calculated based on a path that is formed by pixels. For a certain value of  $\lambda$ , two pixels are called  $\lambda$ -connected if there is a path linking those two pixels and the connectedness of this path is at least  $\lambda$ .  $\lambda$ -connectedness is an equivalence relation.

## 2.6 Level set methods

The level set method was initially proposed to track moving interfaces by Osher and Sethian in 1988 and has spread across various imaging domains in the late nineties. It can be used to efficiently address the problem of

curve/surface/etc. propagation in an implicit manner. The central idea is to represent the evolving contour using a signed function, where its zero level corresponds to the actual contour. Then, according to the motion equation of the contour, one can easily derive a similar flow for the implicit surface that when applied to the zero-level will reflect the propagation of the contour.

The level set method encodes numerous advantages: it is implicit, parameter free, provides a direct way to estimate the geometric properties of the evolving structure, can change the topology and is intrinsic. Furthermore, they can be used to define an optimization framework as proposed by Zhao, Merriman and Osher in 1996. Therefore, one can conclude that it is a very convenient framework to address numerous applications of computer vision and medical image analysis. Furthermore, research into various level set data structures has led to very efficient implementations of this method.

## 2.7 Multi-Scale Segmentation

Image segmentations are computed at multiple scales in scale space and sometimes propagated from coarse to fine scales; see scale-space segmentation. Segmentation criteria can be arbitrarily complex and may take into account global as well as local criteria. A common requirement is that each region must be connected in some sense.

### One-dimensional hierarchical signal segmentation

Witkin's seminal work in scale space included the notion that a one-dimensional signal could be unambiguously segmented into regions, with one scale parameter controlling the scale of segmentation.

A key observation is that the zero-crossings of the second derivatives (minima and maxima of the first derivative or slope) of multi-scale-smoothed versions of a signal form a nesting tree, which defines hierarchical relations between segments at different scales. Specifically, slope extreme at coarse scales can be traced back to corresponding features at fine scales. When a slope maximum and slope minimum annihilate each other at a larger scale, the three segments that they separated merge into one segment, thus defining the hierarchy of segments.

## III. THE PROPOSED CHAN-VESE ACTIVE CONTOUR ALGORITHM

Images are the proper 2D projections of the 3D world containing various objects. To successfully reconstruct the 3D world, at least approximately, the first crucial step is to identify the regions in images that correspond to individual objects. This is the well-known problem of image segmentation. It has broad applications in variety of important fields such as computer vision and medical image processing. Variational methods have been extensively used and studied in image segmentation in the past decade because of their flexibility modeling and various advantages in the numerical implementation. These methods drive one or more initial curve(s), based on gradient and/or region information in the image, to the boundaries of objects in that image. The basic idea of variational methods is to minimize energy. This functional generally depends on the features of the image. The classical way to solve the minimization problem is to solve the corresponding Euler-Lagrange equation. For instance, relatively early, Mumford and Shah introduced a celebrated segmentation model by minimizing an

energy functional that penalizes smoothness within regions and the length of their discontinuity contours. Recently, Chan and Vese developed an active contour without edge model to deal with the problem of image segmentation by using the level-set framework introduced by Osher and Paragios. Tsai et al also independently developed a segmentation method which is similar to it. The active contour methods based on level-set framework have several advantages. First, they can deal with topological changes such as break and merger. Second, intrinsic geometric elements such as the normal vector and the curvature can be easily expressed with respect to the level-set function. Third, this level-set framework can be extended and applied in any dimension. K-means is one of the most popular clustering algorithms. It is simple and fairly fast. K-means is initialized from some random or approximate solution. Each iteration assigns each point to its nearest cluster and then points belonging to the same cluster are averaged to get new cluster centroid. Each iteration successively improves cluster centroid until they become stable. Formally, the problem of clustering is defined as finding a partition of  $D$  into  $k$  subsets such that

$$\sum_{i=1}^n \zeta(t_i; C_j)$$

is minimized, where  $C_j$  is the nearest cluster centroid of  $t_i$ . The quality of a clustering model is measured by the sum of squared distances from each point to the cluster where it was assigned. This quantity is proportional to the average quantization error, also known as distortion. The quality of a solution is measured as:

$$q(R) = 1/n \sum_{i=1}^n \zeta(t_i; C_j)$$

This can be computed from  $R$  as,

$$q(R, W) = \sum_{j=1}^k W_j \sum_{i=1}^d R_{ij}$$

### 3.1 Segmentation Based on Chan-Vese Active Contour

Segmentation was based on the Chan-Vese active contour model. This model is based on the variational information of grayscale intensities of the image. The segmentation algorithm may be summarized as follows:

1. Definition of an initial contour
2. Calculation of average intensity values inside and outside the contour
3. Obtain the next position of the contour
4. Check for stability
5. Determination of the movement of the contour
6. If unstable, iterate from step 2.

### 3.2 Multiphase Chan-Vese Active Contours Without Edges

Simply speaking, in previous two approaches we discussed above, we only try to find one 'active contour'. As we can see from the result, one active contour can only tell us two things: what is the foreground of the image and what is the background. For more details, they fail to tell. Therefore, for any image which has more than

two colors, previous approach cannot distinguish them. They will either get two colors in foreground or catch two colors in background. Following image has several complicated structures: triple junction, quadruple junction, different colors and different shapes. One phase active contours cannot distinguish all objects in the image, while two-phases active contours could achieve this goal.

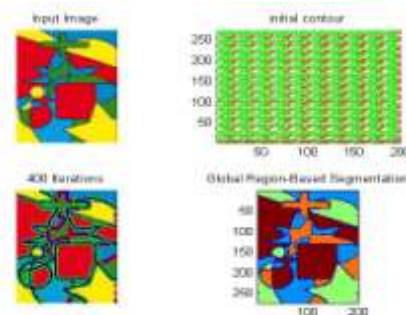


**Figure1: Multiphase Active Contour**

Above result shows that multiphase active contours could distinguish much more objects and automatically detect every edge in the input image. This method can easily handle different complicated topological changes. In this photo image, background is sky and foreground is two red and two yellow flowers. By using multiphase active contour, we can get the segmentation as follows.

#### IV. ALGORITHM IMPLEMENTATION

Ethical approval was obtained and the ultrasound images were taken using a 12MHz linear probe. The images were exported to MATLAB®. The region of interest was chosen and the image was cropped accordingly. Preprocessing of these images was performed to reduce the speckle and enhance the visibility of the structures. This improves the accuracy of the segmentation. The segmented image was then displayed in grayscale with identifiable segments or as a color specific segmented image with an option of the choice of a particular segment for selective processing.

##### 4.1 Preprocessing

The preprocessing had two steps- anisotropic diffusion filtering and contrast enhancement. The anisotropic diffusion filter, the image is convolved with a Gaussian kernel. For implementation in MATLAB®, the nearest neighbor differences are taken for convolution. A diffusion coefficient is calculated. This coefficient varies so as to preferably perform intra-region smoothing rather than inter-region smoothing in spite of the coarser resolution of the convolved image. All maxima in the filtered image have a causative source and no new maxima are created due to anisotropic diffusion. The following filter function  $g$  which prefers high contrast edges over low contrast edges has been used on the image  $I$ :

$$g(\nabla I) = e^{-(\|\nabla I\|/K)^2}$$

The constant  $K$  was experimentally set as 30.

This is followed by contrast enhancement using morphological transforms [6]. Two disk shaped structuring elements of radii 3 and 30 pixels were chosen and bottom-hat and top-hat transforms were applied. This resulted

in the retention of the darker regions and brighter regions smaller than the elements respectively. The dark features within the range created by the two structuring elements are obtained by subtracting the features obtained previously. Similarly, the bright features are also obtained within the same range.

$$I_d = I_{bh_1} - I_{bh_2}$$

$$I_b = I_{bh_2} - I_{bh_1}$$

A rescaling constant  $\alpha$  is taken as 0.5 and the following equation is implemented:

$$I_n = I_0 - \alpha I_d + \alpha I_b$$

This gives the contrast enhanced image after addition of the brighter regions and subtraction of the darker ones.

#### 4.2 Segmentation

Segmentation was based on the Chan-Vese active contour model [8]. This model is based on the variational information of grayscale intensities of the image. The segmentation algorithm may be summarized as follows:

1. Definition of an initial contour
2. Calculation of average intensity values inside and outside the contour
3. Obtain the next position of the contour
4. Check for stability
5. Determination of the movement of the contour
6. If unstable, iterate from step 2

**Mathematical formulation:** Considering  $\Omega$  as an open subset of  $\mathbb{R}^2$ , is the given image. The evolvable curve  $C$  is represented using a Lipschitz function for implementation of the active contour model using level set methods.

$$C = \{(x, y) | \phi(x, y) = 0\}$$

This model is implemented using the level set methods. The image is considered to consist of two regions of piecewise linear intensities representing the region inside the contour and the region outside it. The region inside is the object to be detected. The border of this object is ideally the end point of contour movement. The energy  $F$  for the contour  $C$  is given by

$$F(c_1, c_2, \phi) = \mu \int_{\Omega} \delta(\phi(x, y)) |\nabla \phi(x, y)| dx dy$$

$$+ \nu \int_{\Omega} H(\phi(x, y)) dx dy + \lambda_1 \int_{\Omega} |u_0(x, y) - c_1|^2 H(\phi(x, y)) dx dy$$

$$+ \lambda_2 \int_{\Omega} |u_0(x, y) - c_2|^2 (1 - H(\phi(x, y))) dx dy$$

The first term in this functional represents the energy on the contour, the second term is the length regularization term and the third and fourth terms represent the energy inside the contour and outside it respectively. The minimization of this functional gives the ideal boundary contour. The solution is given by The Heaviside function is regularized in the following manner in order to detect global minima rather than only local minima and also to detect interior boundaries



$$H(z) = \begin{cases} 1 & z > \varepsilon \\ 0 & \text{if } z < -\varepsilon \\ \frac{1}{2} \left( 1 + \frac{2}{\pi} \arctan\left(\frac{z}{\varepsilon}\right) \right) & |z| \leq \varepsilon \end{cases}$$

Curvature is also considered for segmentation in addition to the parameters of the energy functional. Curvature is given

$$\kappa = \frac{\phi_{xx}\phi_y^2 - 2\phi_x\phi_{xy}\phi_y + \phi_x^2\phi_{yy}}{(\phi_x^2 + \phi_y^2)^{3/2}}$$

## V. RESULTS

### Extracting the area of Ulcer affected in a foot using Chen-Vese Active Contour

The result of ulcer affected area in foot is shown below.

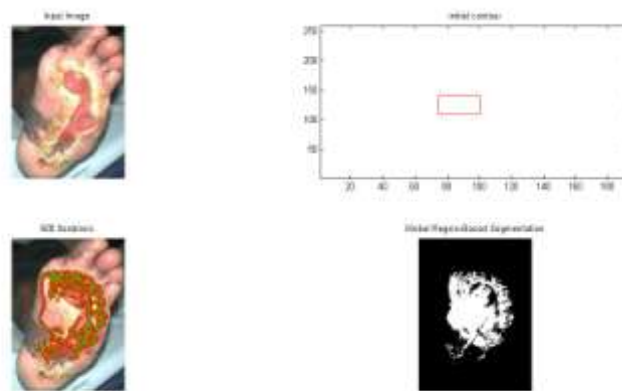


**Figure2: Result of Damaged Area In Diabetic Foot Ulcer**

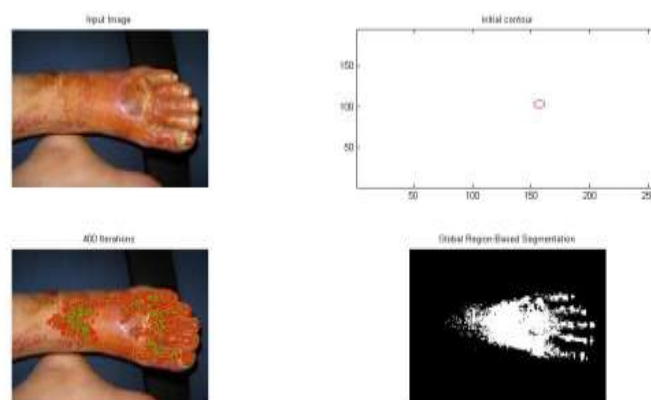


**Figure3: Result Of Ulcer Effected In Lower Part Of Foot**

In the above results the input image shows the ulcer effecting foot. The Chan-veve Active contour performs segmentation and extract the ulcer effected area.

## VI. CONCLUSION

We have counted the number of objects in an image using thresholding along with marker controlled watershed segmentation. The accuracy of the method was tested with various types of images. The method works well in both same color and different color objects. The method gives better result with high definition images. Another shortcoming of the method is- that when the particles are of different tones of colors, it takes bright objects as object and darks objects are considered as background. Future analysis and work can be done to overcome the issue. If objects are of same color tone test result gives almost perfect counting.

## REFERENCES

- [1] I. Maglogiannis, S. Pavlopoulos, D. Koutsouris, "An integrated computer supported acquisition, and characterization system for pigmented skin lesions in dermatological images," *IEEE Transactions on Information Technology in Biomedicine*, 9:86-98, March 2005.
- [2] H. Oduncu, A. Hoppe, M. Clarck, R. J. Williams, K. G. Harding, "Analysis of skin wound images using digital color image processing: a preliminary communication," *The International Journal of Lower Extremity Wounds*, 3(3):151-156, 2004.
- [3] A. S. Tarallo, A. Gonzaga, M. A. C. Frade. "Artificial neural networks applied to the segmentation and classification of digital images of cutaneous ulcers," In: *IEEE 7th International Conference on Bioinformatics and Bioengineering*, Boston, MA, IEEE Press, vol. 1, p. 1-1, 2007.
- [4] E. A. G. Dorileo, M. A. C. Frade, A. M. Roselino, R. M. Rangayyan, P. M. de Azevedo Marques, "Color image processing and content-based image retrieval techniques for the analysis of dermatological lesions", In: *Proc. 30th Annual International Conference of the IEEE Engineering in Medicine and Biology Society*, August 2008, Vancouver, BC, Canada. pp 1230-1233.
- [5] H. Wannous, S. Treuillet, Y. Lucas, "Supervised tissue classification from color images for a complete wound assessment tool", *Proceedings of the 29th Annual International Conference of the IEEE EMBS*, Lyon, France, August 2007, pp 6031-6034.
- [6] D. Tschumperlé, R. Deriche, "Vector-valued image with PDE's: a common framework for different applications", *IEEE Transactions on Pattern Analysis and Machine Intelligence*, 27(4): 506-517, 2005.
- [7] R. C. Gonzalez, R. E. Woods, "Digital Image Processing", Prentice-Hall, Upper Saddle River, NJ, 2nd Edition, 2002.
- [8] R. M. Rangayyan, *Biomedical Image Analysis*. CRC Press, Boca Raton, FL, 2005.
- [9] W. S. Rasband, *ImageJ*, U. S. National Institutes of Health, Bethesda, MD, <http://rsb.info.nih.gov/ij/>, 1997-2009. [10] T. W. Ridler, S. Calvard, "Picture thresholding using an iterative selection method", *IEEE Transactions on Systems, Man, and Cybernetics*, SMC-8(8): 630-632, 1978.
- [11] C. Serrano, B. Acha, T. Gómez-Cía, J. Acha, L. Roa, "A computer assisted diagnosis tool for the classification of burns by depth of injury", *Burns*, 31(3):275-281, 2005.
- [12] I. Fondón, C. Serrano, B. Acha, "Color-texture image segmentation based on multistep region growing", *Optical Engineering*, 45(5):057002:1-9, May 2006.
- [13] B. Acha, C. Serrano, J. I. Acha, L. M. Roa, "Segmentation and classification of burn images by color and texture information", *Journal of Biomedical Optics*, 10(3):034014, 2005.